Mass Spectrometry Reveals that Oxysterols are Secreted from Non-Alcoholic Fatty Liver Disease Induced Organoids

Kristina Sæterdal Kømurcu[a,b], Ingrid Wilhelmsen[b], James L Thorne[c], Stefan Johannes Karl Krauss[b], Steven Ray Haakon Wilson[a,b], Aleksandra Aizenshtadt[b] and Hanne Røberg-Larsen[a,b]*

[a]Department of Chemistry, University of Oslo, P.O. Box 1033 Blindern, 0315 Oslo, Norway,
[b]Hybrid Technology Hub - Centre of Excellence, Institute of Basic Medical Sciences, University of Oslo, P.O. Box 1110 Blindern, 0317 Oslo, Norway
[c] School of Food Science and Nutrition, University of Leeds, Leeds LS2 9JT, United Kingdom

*Corresponding author: E-mail: hannero@kjemi.uio.no. Telephone: +47 22 85 5587.

Abstract

Oxysterols are potential biomarkers for liver metabolism that are altered under disease conditions such as non-alcoholic fatty liver disease (NAFLD). We here apply sterolomics to organoids used for disease modeling of NAFLD. Using liquid chromatography-mass spectrometry with on-line sample clean-up and enrichment, we establish that liver organoids produce and secrete oxysterols. We find elevated levels of 26-hydroxycholesterol, an LXR agonist and the first oxysterol in the acidic bile acid synthesis, in medium from steatotic liver organoids compared to untreated organoids. Other upregulated sterols in medium from steatotic liver organoids are dihydroxycholesterols, such as 7α,26–dihydroxycholesterol, and 7α,25-dihydroxycholesterol. Through 26-hydroxycholesterol exposure to human stem cell-derived hepatic stellate cells, we observe a trend of expressional downregulation of the pro-inflammatory cytokine CCL2, suggesting a protective role of 26-hydroxycholesterol during early-phased NAFLD disease development. Our findings support the possibility of oxysterols serving as NAFLD indicators, demonstrating the usefulness of combining organoids and mass spectrometry for disease modeling and biomarker studies.

Keywords: Liquid Chromatography, NAFLD, Mass Spectrometry, Organoids, Oxysterols

31 **Graphical abstract:**

32

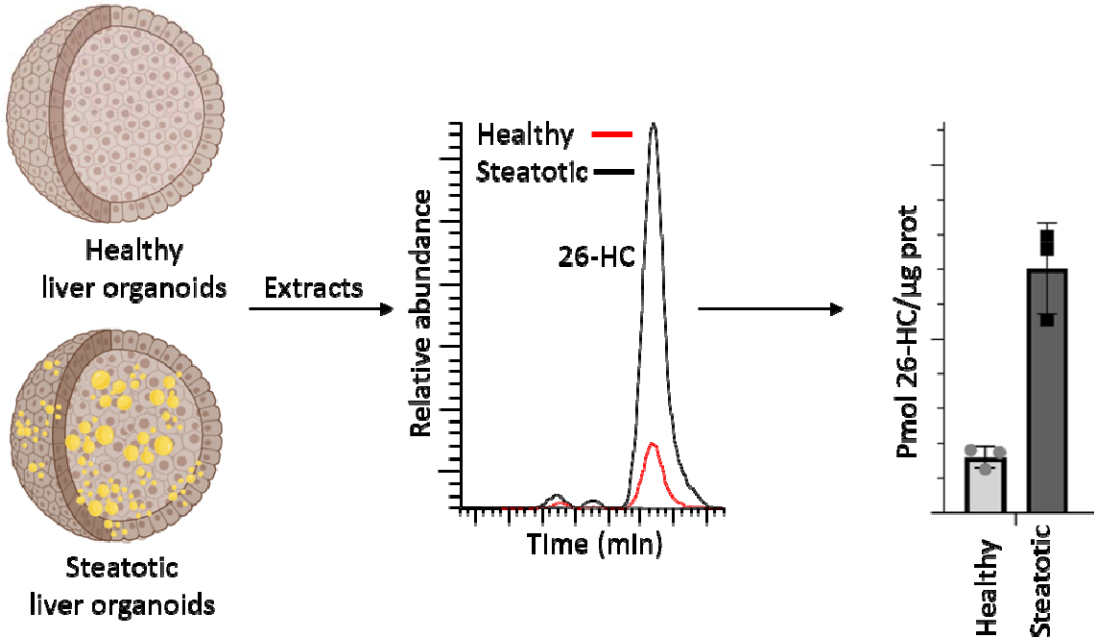

33

34

35

36

37

38

39

40

41

42

INTRODUCTION

Non-alcoholic fatty liver disease (NAFLD) is a heterogeneous disease related to the accumulation of high levels of lipids in the liver [1, 2]. Studies estimate the pooled global prevalence of all forms of NAFLD to be 30% [3]. NAFLD is closely interlinked with obesity, but studies also show that diabetes increases the risk of developing more severe stages of NAFLD [2]. NAFLD is divided into stages according to disease progression (*Figure 1*), starting with the benign steatotic stage where the liver has begun to build up lipids before evolving to non-alcoholic steatohepatitis (NASH), where inflammation occurs. As a consequence, tissue scarring (fibrosis) occurs until it reaches cirrhosis, the stage where liver function is significantly severed. Disease progression can cause liver cancer (hepatocellular carcinoma (HCC)) and liver failure ultimately requiring liver transplantation [1].

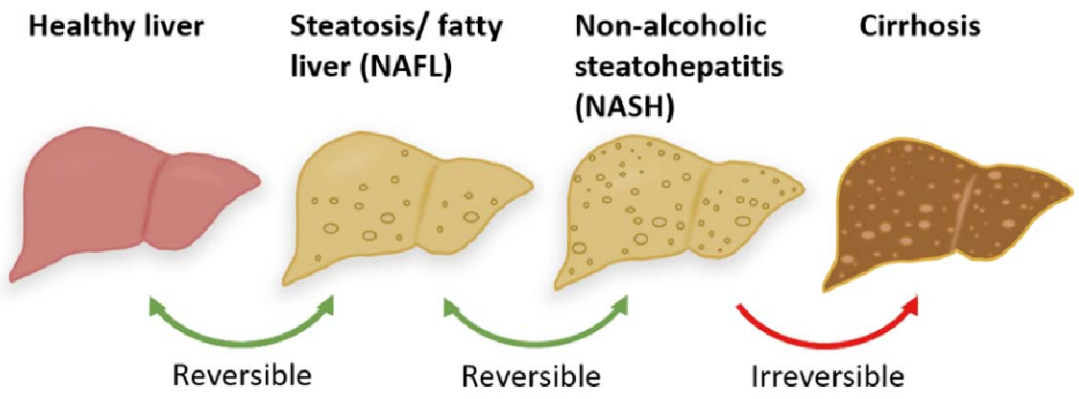

Figure 1. The stages of NAFLD progression. In the first stage, steatosis, the liver accumulates higher levels of fat (fatty liver). The next stage is NASH, where the degree of fibrosis (tissue scarring) is increasing. When the tissue scarring is severe, the liver function is altered (cirrhosis) and liver transplantation is often needed.

Today, the most specific and common test to diagnose and stage NAFLD is a liver biopsy. The use of ultrasound-based approaches or non-invasive diagnostic methods based on biomarkers has pitfalls, such as low sensitivity in early stages leading to an inability to assess the severity of the disease [4]. New biomarkers to increase understanding of disease onset, progression, and diagnosis are needed.

64 Due to differences between animal models and human physiology - rodent models don't fully
65 reproduce human liver metabolism [5], both human liver spheroids and liver organoids, are
66 increasingly used for NAFLD modeling and biomarker discovery [6]. While liver spheroids can be
67 described as 3D clusters of differentiated cells without recapitulation of elements of tissue-like
68 structure, liver organoids are developed from human pluripotent stem cells (PSC)[7].
69 Additionally, stem-cell-derived 2D monocultures of key effector cells can be used for modeling
70 NAFLD in an even more simplified system.

71 Cholesterol derivates have received attention as potential biomarkers of NAFLD [8-10].
72 Oxysterols are oxidized forms of cholesterol (Figure 2) and are involved in a plethora of
73 biochemical processes and diseases [11]. In the context of NAFLD, oxysterols are regulators of
74 the liver x-receptor (LXR) [12], a key modulator in NAFLD [13]. Chronic LXR activation
75 contributes to the development of steatosis, where dysregulation of oxysterols metabolism may
76 affect the severity of NAFLD toward NASH [14]. Ikegami et al. found elevated levels of 25-
77 hydroxycholesterol (HC) and 26-HC (also known as 27-HC [15]) in serum samples from NAFLD
78 patients [9]. Raselli et al. found elevated levels of 24- and 7-hydroxylated oxysterols in liver
79 biopsy samples of patients with NASH [10]. Studying murine models of NASH Raselli et al found
80 elevated levels of 24-HC and 7α-hydroxycholeste-4-en-3-one, but these findings differ from
81 studies of the human liver. Hence, while oxysterols are implicated in NAFLD progression and
82 may serve as biomarkers, their exact role in disease initiation and progression in humans
83 remains unclear. Specifically, the effect of oxysterols on liver non-parenchymal cells, essential
84 for the progression of NAFLD, including hepatic stellate cells (HSCs), is unexplored. Hence,
85 studying oxysterols in organoid models of NAFLD may add to our understanding of this
86 metabolites group.

87 Oxysterols are a highly challenging group of analytes to measure and elucidate, even when
88 applying high-performance liquid chromatography-mass spectrometry (LC-MS). Many oxysterols
89 are isomers, requiring high chromatographic resolution before MS. In addition, oxysterols are
90 difficult to charge, resulting in poor sensitivity when applying conventional electrospray
91 ionization before MS detection. Therefore, sensitive LC-MS requires oxysterols to be derivatized

by introducing chargeable groups. To the authors´ knowledge, oxysterols have hitherto not been analysed in human liver organoids and *in vitro* models of NAFLD.

We here introduce mass spectrometric analysis of oxysterols on human liver spheroids and organoids with the goal of assessing correlations between levels of specific oxysterols and early stages of NAFLD (steatosis).

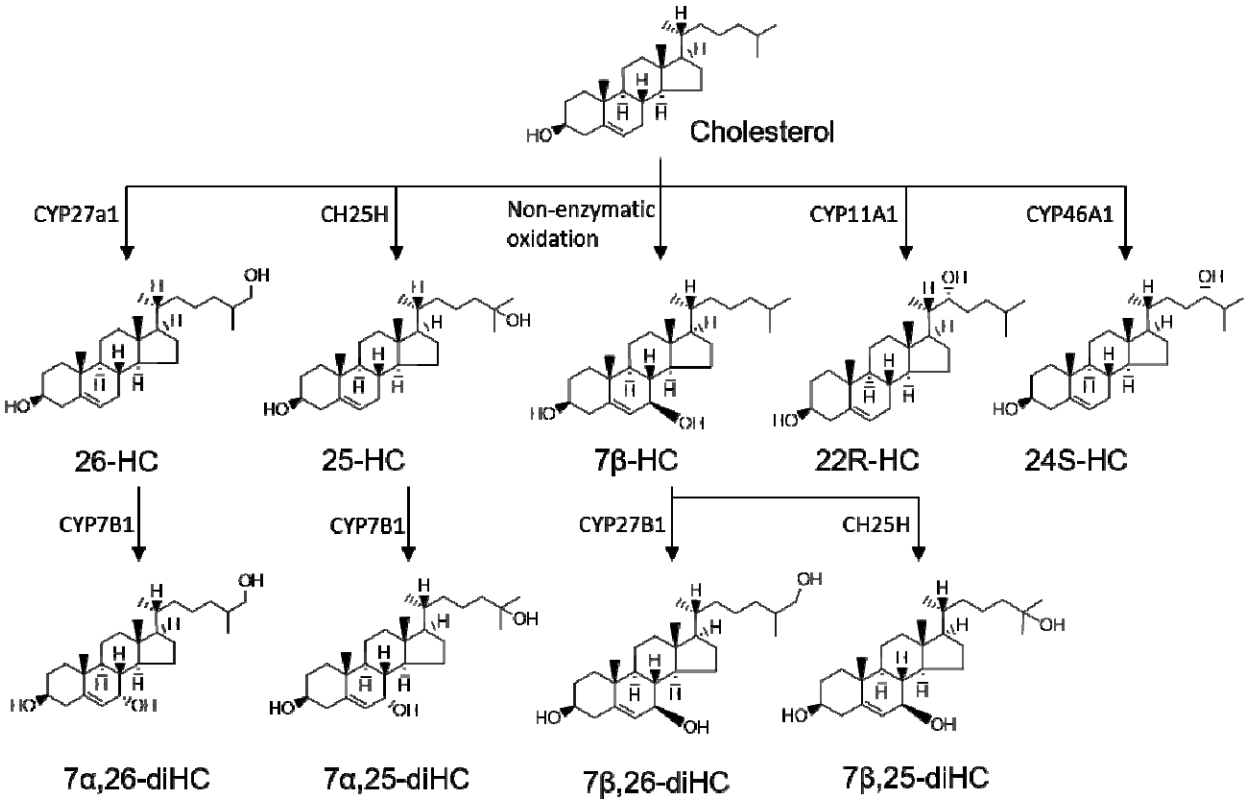

Figure 2. Oxysterol formation. Cholesterol is oxidized to form oxysterols, via cytochrome P450 (CYP) enzymes.

99 **EXPERIMENTAL**
100

101 **Generation of human primary hepatic spheroids (PHH)**

102 Cryopreserved primary human hepatocytes (PHH) (Lonza, catalogue no.HUCPG, lot
103 HUM180201A (PHH_1) and Gibco, catalogue no. HMCPMS, lot HU8287 (PHH_2)) were thawed
104 in the Hepatocytes thaw media (Gibco, catalogue no. CM7500) according to the manufacturer's
105 protocol. Uniform PHH spheroids were created by aggregation in-house-made agarose
106 microwells - a format in which PHH showed stable functionality over at least 7 days as described
107 before[7]. Briefly, cells were plated into microwells at the concentration of 1000 viable cells per
108 microwell and were centrifuged at 100 g for 2 min. For the first 3 days PHH was cultured in the
109 Williams E medium (Thermo Fisher Scientific, catalogue no. A1217601) supplemented with 7 %
110 FBS (Thermo Fisher Scientific, catalogue no. 41400045), 2 mM L-glutamine (Thermo Fisher
111 Scientific, catalogue no. 35050038), 10 µg/ml insulin, 5.5 µg/ml transferrin, 6.7 ng/ml sodium
112 selenite (Thermo Fisher Scientific, catalogue no. 41400045) and 0.1 µM dexamethasone (Sigma
113 Aldrich, catalogue no. D4902). From day 4 onwards, the FBS concentration was gradually
114 decreased to 1 % (v/v).

115 **Generation of human induced PSC/human embryonic stem cell-derived human-like**
116 **hepatocytes (HLC)**

117 Human induced pluripotent stem cells (hiPSC)(HLC_1: WTSIi013-A; HLC_3: WTC-11, Coriell
118 Institute for Medical Research) and human embryonic stem cells (hESC) (HLC_2: H1) were
119 cultured in E8 media (Thermo Fisher Scientific, catalogue no. A1517001) on plates coated with
120 0.1 % (v/v) Geltrex (Thermo Fisher Scientific, catalogue no. A1413201) in a humidified 37 °C, 5
121 % CO_2 incubator. Quality control, performed after the thawing of cells, including flow cytometry,
122 real-time polymerase chain reaction, immunofluorescent imaging for pluripotency markers, and
123 karyotyping.

124 HLC was generated using an protocol established in our laboratory [16]. Briefly, iPSC was
125 differentiated toward definitive endoderm with the subsequent treatment with 10 ng/mL FGF2
126 (Peprotech, catalogue no. 100-18B) and 20 ng/mL BMP4 (Peprotech, catalogue no. 120-05) in

127 IMDM/F12 medium supplemented with 1% (v/v) N-2 (Thermo Fisher Scientific, catalogue no.
128 17502-048), 1% (v/v) B-27 minus vitamin A (Thermo Fisher Scientific, catalogue no. 12587010)
129 and 1% (v/v) lipid concentrate, then with 5 µM A8301 (Stem Cell Technologies, catalogue
130 no.72022), 20 ng/mL HGF (Peprotech, catalogue no. 100-39H), 20 ng/mL BMP4, 1% (v/v) B-27
131 with vitamin A for 3 more days and with 25 ng/mL HGF, 1% (v/v) DMSO for another 5 days.
132 Obtained hepatic progenitors (day 12) were detached and aggregated in the agarose U bottom
133 microwells in the presence of 25 ng/mL HGF, 0.1 µM Dexamethasone, 0.5% (v/v) ITS, 0.1% (v/v)
134 lipids concentrate, 100 µM Ascorbic acid-2 phosphate (AAP), 1% (v/v) B-27 (without vitamin A)
135 and 1% (v/v) N-2. After the formation of spheroids at day 13, media was replaced with William's
136 E media, supplemented with 5% (v/v) FBS, 20 ng/ml HGF and 10 ng/ml Oncostatin M
137 (Peprotech, catalogue no. 300-10), 1% (v/v) ITS, 100 µM AAP, 0.1 µM dexamethasone.
138 Organoids were cultured in microwells in William's E media, supplemented with 1% (v/v) ITS, 0.1
139 µM Dexamethasone, 20 ng/ml Oncostatin M and 1% (v/v) MEM Non-Essential Amino Acids
140 Solution (Thermo Fisher Scientific, catalogue no. 11140050), for another 10 days.

141 **Steatosis induction**

142 To induce hepatic steatosis, PHH or HLC were incubated for 48 h in the serum-free William's E
143 media, supplemented with 10 mM fructose, and saturated (palmitic acid, 250 µM) and mono-
144 unsaturated (oleic acid, 250 µM) free fatty acids in ratio 1:1, termed below as steatotic
145 conditions [7]. Incubation was performed in ultra-low attachment 24 wells-plate, with 20-30
146 organoids per well filled with 500 µl of control or steatotic media.

147 **Differentiation of human iPSC-/ hESC-derived hepatic stellate cells**

148 2D cultures of human stem cell-derived hepatic stellate cells (sc-HSCs) were generated using
149 modifications of previously published protocols [17, 18]. Human PSCs were seeded as single
150 cells in a 1:4 ratio on plates coated with 1 % (v/v) GelTrex matrix (Thermo Fisher Scientific) and
151 pretreated with 10 µM Rock inhibitor (STEMCELL Technologies). The sc-HSCs differentiation
152 protocol was initiated by the incubation with DMEM/F12 GlutaMax™ medium (Gibco, catalogue
153 no. 31331-093) supplemented with 1 % (v/v) MEM non-essential amino acids (Gibco, catalogue
154 no. 11140050),1 % (v/v) B-27™ supplement (Gibco, catalogue no. 17504044), 100 ng/mL activin

155 A (Peprotech, catalogue no. 120-14P), 3 µM CHIR99021 (Tocris Bioscience, catalogue no. 4423)
156 and 20 ng/mL BMP-4 (Peprotech, catalogue no. 120-05) for 24 hours on day 0 of the
157 differentiation protocol. Mesodermal progenitors obtained in this stage were incubated in
158 DMEM/F12 GlutaMax™ medium supplemented with 1 % (v/v) MEM non-essential amino acids,
159 1 % (v/v) B-27™ supplement, 1 % (v/v) Insulin-Transferrin-Selenium (Gibco, catalogue no.
160 41400045), 2.5 µM Dexamethasone (Sigma-Aldrich, catalogue no. D4902-100mg) and 100 µM 2-
161 Phospho-L-ascorbic acid trisodium salt (Sigma-Aldrich, catalogue no. 49752) including 20 ng/mL
162 BMP-4, and, to induce a liver mesenchymal submesothelial phenotype. Next 20 ng/mL FGF-1
163 (Peprotech, catalogue no. 100-17A) and 20 ng/mL FGF-3 (R&D Systems, catalogue no. 1206-F3-
164 025) were added on days 3-11. On days 6-12, B-27™ supplement was replaced with 1 % (v/v)
165 Fetal Bovine Serum (Gibco, catalogue no. 26140079) and 100 µM Palmitic Acid (Sigma-Aldrich,
166 catalogue no. P5585) and 5 µM Retinol (Sigma-Aldrich, catalogue no. R7632) was added to the
167 media to induce a fetal HSC-like phenotype.

168 **sc-HSC activation and treatment with cholesterol and oxysterols 25-HC and 26-HC**

169 After differentiation, sc-HSCs were treated with 100 nM 25-HC, 100 nM 26-HC (both from
170 Sigma-Aldrich, St. Louis, MA, USA), or 50 µM cholesterol (Promega, catalogue no. J322A) both
171 with and without 25 ng/mL TGF-β1 (Abcam, catalogue no. ab50036) for 48 hours. Samples were
172 then collected after detachment with Trypsin-EDTA solution (Sigma-Aldrich, catalogue no.
173 T4049-100ML) and snap frozen at -80 °C until RNA extraction and real-time quantitative
174 polymerase chain reaction (RT-qPCR) analysis. Biological triplicates were collected for each
175 condition.

176 **RNA extraction and real-time quantitative polymerase chain reaction.**

177 RNA was isolated using RNeasy Micro kit (Qiagen) or TRIzol reagent (Thermo Fisher) according
178 to the manufacturer's protocol. RNA concentration and purity were determined using
179 NanoDrop ND-1000 spectrophotometer (Thermo Fisher Scientific). cDNA was synthesized using
180 High-Capacity cDNA Reverse Transcription Kit (Thermo Fisher Scientific, catalogue no. 4368814).
181 Gene expression analysis was performed using a TaqMan Universal mix on a TaqMan ViiA7 Real-
182 Time PCR System. Used primers are listed in the Supporting Information table 1. GAPDH was

183 used as endogenous control. The level of expression of genes of interest was quantified by ddCt
184 with to HLC differentiated from the WTSIi028-A iPSC line (HLC_1), and with normalization to
185 control organoids. Data represent two donor PHH samples, and HLC differentiated from 3 cell
186 lines.

187 **Immunofluorescence and lipids detection**

188 Organoids were fixed in 4 % (w/v) PFA for 30 min on the orbital shaker. Each step in the
189 protocol was followed by 3 washings (each 5 min) in DPBS using an orbital shaking.
190 Permeabilization and blocking were performed by incubation in PBS with 1 % (w/v) BSA (Sigma
191 Aldrich), 0.2 % (v/v) Tritox-X100 (Sigma Aldrich), and 0.5 % (v/v) DMSO at RT for 2 h on the
192 orbital shaker. Staining with primary antibodies was performed for 24 h (at 4 °C) with
193 subsequently 2 h incubation with secondary antibodies (Jackson ImmunoResearch, West Grove,
194 PA) diluted with 1 % (w/v) BSA, 0.1 % (v/v) Tritox-X100 in PBS. Primary antibodies (Ab) used in
195 this study: rabbit polyclonal Ab to human serum albumin (Abcam, catalogue no.ab2406, 1:400),
196 goat polyclonal Ab to PDGFR-β (R&D Systems, catalogue no. AF385), rabbit monoclonal Ab to
197 NCAM1 (Abcam, catalogue no. ab75813), mouse monoclonal Ab to Vimentin (Abcam, catalogue
198 no. ab8978); secondary Ab used in this study: Cy™3 AffiniPure Donkey Anti-Rabbit IgG (H+L)
199 (catalogue no.711-165-152, 1:400), Alexa Fluor® 647 AffiniPure Donkey Anti-Mouse IgG (H+L)
200 (catalogue no.715-605-150, 1:400) (all secondary Ab are from Jackson ImmunoResearch).
201 Nuclear counterstaining was performed with 1 µg/mL Hoechst 33258 (Sigma Aldrich) for 5 min
202 at RT. Neutral lipids were stained using HCS LipidTOX™Red Neutral Lipids (excitation/emission
203 maxima ~577/609 nm, Thermo Fisher Scientific, catalogue no. H34476) or Nile Red (Sigma
204 Aldrich).

205 Confocal microscopy was performed on a Zeiss 700 laser scanning confocal microscope.
206 Confocal microscope using standard filter sets and laser lines with a 40x oil immersion objective.
207 Images were acquired using Zen software (Zeiss) as Z-stacks with 2 µm spacing between stacks
208 and Dragonfly software with 0.5 µm spacing correspondingly. The confocal images were
209 analysed using Fiji software [19]. Confocal images are displayed as a resulting Z-stack of half of
210 the spheroid.

211

212

213 **Detection of vitamin A in HSCs**

214 Vitamin A storage was indirectly determined by imaging autofluorescence in the stem cell-
215 derived HSC under UV light excitation. Cells were imaged using a 10X magnification objective on
216 an Axioscope fluorescent microscope (Zeiss, Jena Germany).

217 **LC-MS analysis**

218 **Chemicals**

219 Methanol (MeOH, Hipersolv), acetonitrile (ACN, LC-MS grade), and sodium hydroxide (NaOH)
220 were from VWR (Radnor, Pa, USA), and type 1 water was from a Millipore integral system
221 (Millipore, Billerica, MA, USA). Girard T reagent, cholesterol oxidase from *Streptomyces sp.*,
222 KH_2PO_4, formic acid (FA, HPLC-grade, 98 %), 22R-HC, 25-HC, and cholesterol-25,26,27-$^{13}C_3$ were
223 all purchased from Sigma-Aldrich (St. Louis, MA, USA). A stock solution of 50 mM phosphate
224 buffer with 0.03 mg/mL cholesterol oxidase (pH adjusted to 7 with 1 M NaOH) was stored at –
225 80 °C; fresh buffer was thawed before each use. Glacial acetic acid was from Merck (Merck
226 KGaA, Darmstadt, Germany). 7β,25-diHC, 7α,25-diHC, 7α,24S-diHC, 7α,26-diHC, 7β,26-diHC,
227 24S-HC, 26-HC, 7α,25-diHC-d_6, 7α,26-diHC-d_6, 25-HC-d_6 and 26-HC-d_6 were purchased from
228 Avanti Polar Lipids (Alabaster, AL, USA). All stock solutions of standards or internal standard (95-
229 100 µM) were prepared in 2-propanol (LC-MS-grade, Rathburn Chemicals Ltd., Walkerburn,
230 Scotland, UK) and stored at - 20 °C.

231 **Calibration solutions**

232 Working solutions of 1 nM standard mixture A (7β,25-diHC, 7α,25-diHC and 7α,24S-diHC), 1 nM
233 standard mixture B (7α,26-diHC, 7β,26-diHC, 22R-HC, 25-HC. 24S-HC, and 26-HC) and 1.5 nM
234 internal standard mixture (7α,25-diHC-d_6, 7α,26-diHC-d_6, 25-HC-d_7 and 26-HC-d_7) were diluted
235 from 95-100 µM stock solutions. Calibration *solutions* in the concentration range of 50-500 pM
236 (200 pM internal standard) were made of 100 µL internal standard mixture, 37-370 mL standard
237 mixture (A or B), 100 µL media (for matrix matching) and 88 µL of 1 nM cholesterol-25,26,27-

238 $^{13}C_3$ (120 pM final concentration, for autoxidation monitoring). Samples were evaporated to
239 dryness and resolved in 20 µL IPA before Girard T-derivatization. New calibration solutions were
240 made for each assay.

241 **Liver organoid samples**

242 For each cell line three replicates were collected and again divided into three technical
243 replicates, providing 9 replicates for each cell line. Approximately 90 µL of the organoid medium
244 was mixed with 100 µL internal standard (200 pM) and 88 µL of 1 nM cholesterol-25,26,27-^{13}C
245 (120 pM final concentration) for autooxidation monitoring [20]. Samples were evaporated to
246 dryness and redissolved in 20 µL IPA before Girard T-derivatization. All samples were stored at 4
247 °C and analysed within 3 weeks.

248 **Sample preparation – Girard T**

249 Oxysterols were derivatized by the procedure described by Griffith et al [21] with modifications
250 as described by Roberg-Larsen et al [22] (Figure 3). Briefly, 200 µL of aliquoted cholesterol
251 oxidase solution was added to each sample/standard and incubated at 37 °C for one hour. A
252 mixture of 500 µL MeOH, 15 µL glacial acetic acid, and 15 mg Girard T was added to each
253 sample followed by incubation overnight in darkness. Samples were then stored at 4 °C and
254 analysed within 2-3 weeks.

255

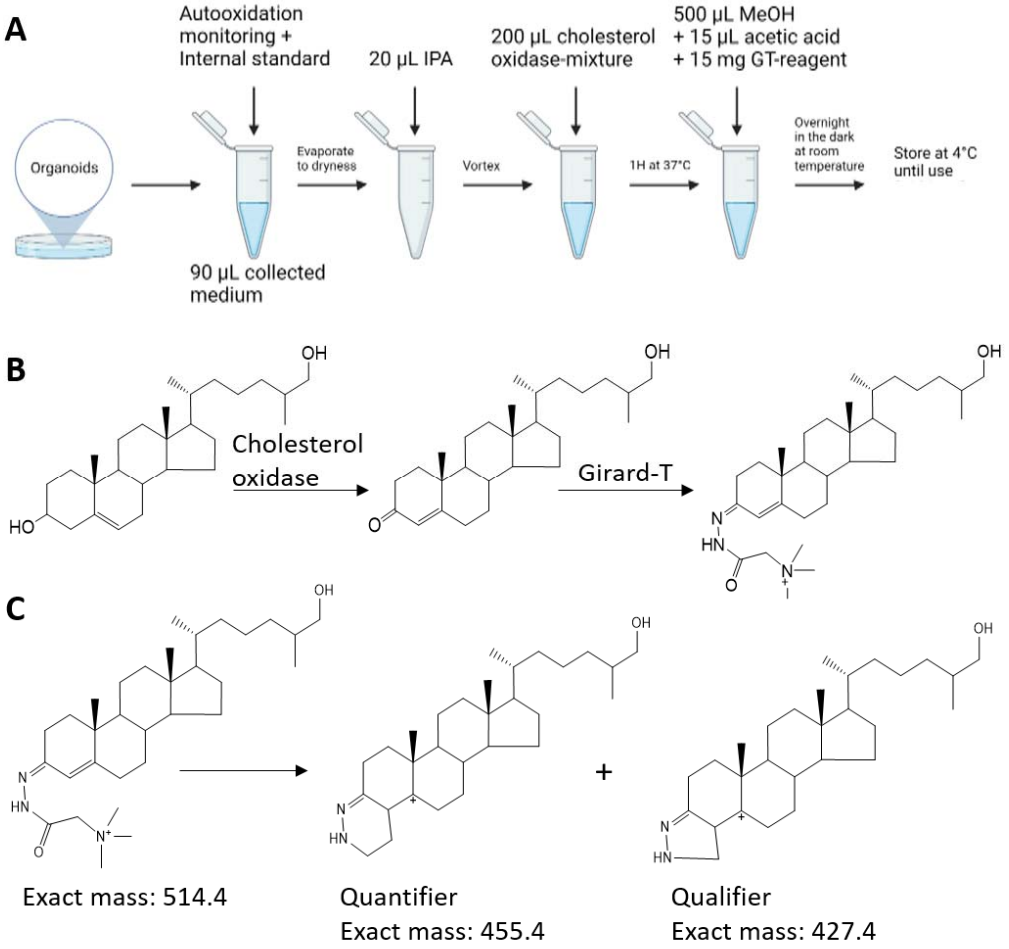

Figure 3. *Sample preparation of oxysterols. Medium is collected from the organoid wells and sample preparation, including Girard T-derivatization, is performed according to the process shown in A. B) The derivatization of 26-HC with Girard T reagent. The OH-group is first oxidized by cholesterol oxidase, before the newly formed carbonyl group reacts with the Girard T reagent, forming a Girard T-derivate. C) The precursor oxysterol-Girard T is fragmented in the MS into the quantifier (m/z =* 455.4) and the qualifier (*m/z = 427.4*).

Liquid chromatography-mass spectrometry system

A previously established method for the hydroxycholesterols 22R-HC, 25-HC, 24s-HC and 26-HC was altered to also include the five dihydroxycholesterols 7α,25-diHC, 7β,25-diHC, 7α,24S-diHC, 7α,26-diHC and 7β,26-diHC [23]. Mobile phase A was 0.1 % FA in type 1 H_2O; B was 0.1 FA in MeOH, and C was 0.1 % FA in ACN. Compared to the aforementioned method, the step gradient was extended with a 7 min step of MP composition 62/14/24 (v/v/v, A/B/C) at the start of separation to achieve separation of the diHCs before an increase in MP strength to 56/14/30

270 (v/v/v, A/B/C). A 2.5 min wash step followed using a MP composition of 50/50 (v/v, B/C). The
271 total method runtime, including on-line sample clean-up and column conditioning, was 21 min.
272 Aliquots of 80 µL of derivatized samples were loaded onto an automated filtration and filter
273 backflush solid phase extraction (AFFL)-system, as described in Solheim et al [23] (Figure 4).
274 Briefly, in the "load"-position, injected samples are filtered on-line before focusing of analytes
275 to an on-line HotSep C18 SPE column (Teknolab, Ski, Norway). Loading is performed at a flow
276 rate of 0.5 µL/min, using mobile phase A, by a Hitachi L-7110 pump (Merck). Non-retained
277 compounds (e.g. excess Girard-T reagent) are sent to waste. When the valve is switched to the
278 "inject" position, the retained compounds are eluted from the SPE and subsequently separated
279 on an ACE SuperPhenyl Hexyl (2.1 mm ID, 150 mm, 2.5 µm d_p core-shell particles)-column from
280 Advanced chromatography technologies LTD, Aberdeen, UK (column temperature set to 55 °C)
281 using a Dionex UltiMate 3000 UHPLC-system with a flow rate of 0.7 mL/min (pump 2). A TSQ
282 Vantage triple quadrupole mass spectrometer (Thermo Fisher Scientific, Waltman, MS, USA)
283 operated in selected reaction mode (SRM) was used for MS-analyses; see Supporting
284 Information *Table 1* for MS parameters. Xcalibur software (Thermo) was used for peak
285 integrations.

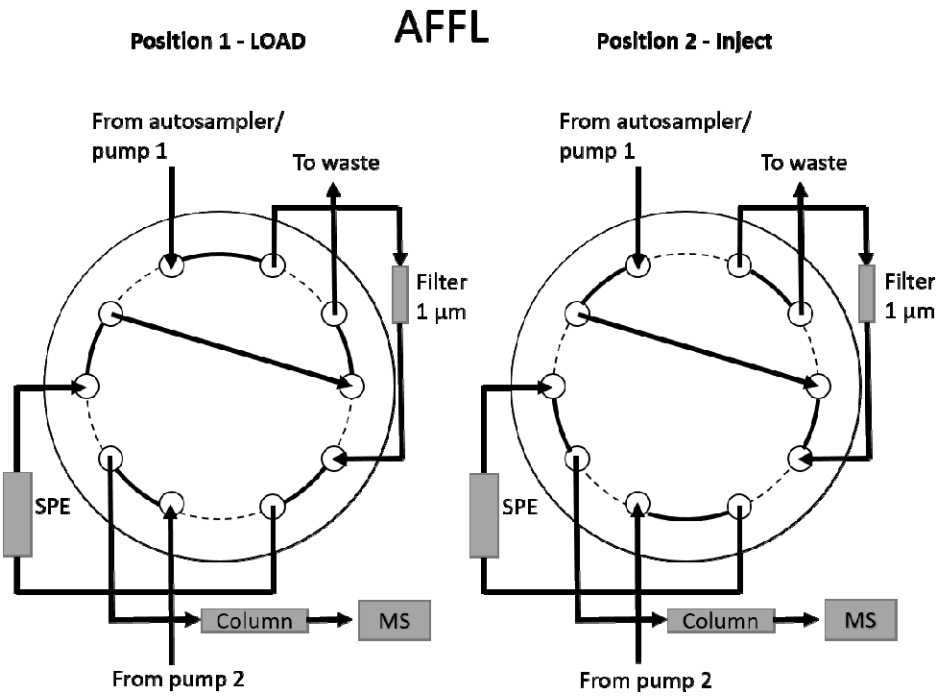

286

287 *Figure 4 The AFFL-system. Illustration of the automated filtration and filter backflush solid phase extraction system (AFFL),*
288 *coupled on-line with LC-MS.*

289

290 **Method evaluation**

291 The method was evaluated at three different concentration levels for both intra-day and inter-
292 day precision, using spiked organoid medium. For intra-day evaluation, 6 replicates for low
293 concentration (50 pM), medium concentration (200 pM), and high concentration (500 pM) were
294 analysed and relative standard deviation was calculated. One-way ANOVA was used to calculate
295 the inter-day-precision (intermediate precision) based on three replicates of each of the three
296 concentration levels prepared and analysed on 4 different days. The limit of quantification is
297 defined as 10 times the S/N and the limit of detection as 3 times S/N, where the ratios for each
298 peak are defined by XCalibur (set to INCOS Noise). No carry-over was observed.

299 **Calculations and statistics**

300 Statistical analyses and graph generation were performed using GraphPad PRISM 9 (GraphPad
301 Software Inc.). For qPRC-analysis, a two-tailed, paired *t*-test was applied for the comparison of

302 two groups. For more than two groups, a one-way ANOVA analysis was applied. For LC-MS
303 results, reported calculations are normalized against the measured protein amount in the
304 corresponding organoid well and reported in pmol per µg protein. When comparing oxysterol
305 levels from steatotic to control organoid samples, a multiple unpaired t-test with Welch
306 correction was used. All data are presented as mean ± SD.

307

308 ## RESULTS AND DISCUSSION

309

310 **Chromatographic system**

311 Oxysterols are isomers with highly similar MS fragmentation, requiring chromatographic
312 separations before detection. By modifying our sterolomics platform [23, 24], we were able to
313 separate and quantify four hydroxycholesterol isomers (22R-HC, 24S-HC, 26-HC, and 25-HC) and
314 five dihydroxycholesterol isomers (7α,25-diHC, 7β,25-diHC, 7α,24S-diHC, 7α,26-diHC and 7β,26-
315 diHC) in 21 minutes, including on-line SPE sample clean-up to remove excess derivatization
316 reagent (0.12 M or 20 mg/mL) and cell medium (Figure 5). Using a phenylhexyl stationary phase
317 we observed no peak splitting of *syn/anti* isomers of post-derivatized oxysterols, an issue often
318 encountered with conventional RPLC stationary phases [21]. The method was evaluated in the
319 range of 50-500 pM for each of the nine analytes (Supporting information *Table 2*). All standard
320 solutions were added cell medium used for organoids before sample preparation for matrix
321 matching. Intra-day RSD values were <28 % for "high" concentrations and < 17% for "middle"
322 concentrations for all HC and diHC. For "low" concentrations, all RSDs were below 22 % except
323 7α,24S-diHC (RSD= 44%). The inter-day RSD values were < 20% for the HCs at all concentrations.
324 For the diHCs inter-day RSDs were higher, ranging from 8% to 20% (7β,25), 12%-27% (7α,25),
325 17-41 % for 724S, 25-38 % (7β,26) and 31-48 % (7α,26). We experienced two peaks for each of
326 the dihydroxycholesterols in standards, with the latter peak being smaller, but the ratio
327 between the peaks was consistent. The additional peaks co-eluted with the major peak of
328 another dihydroxycholesterols, e.g. the latter peak for 7β,25-diHC co-eluted perfectly with
329 7β,26-diHC under all chromatographic conditions, implying that it could be due to impurities in
330 the standard as seen earlier [24]. Hence, we found it adequate to make two calibration curves
331 avoiding the impact of impurities from the standards. R^2 values were > 0.97 for all analytes. The
332 chromatographic resolution ranged from 0.8-1.3 between the isomers. Taken together, the
333 sensitivity, precision, and resolution were considered satisfactory for introducing sterolomics
334 and organoid analysis.

335

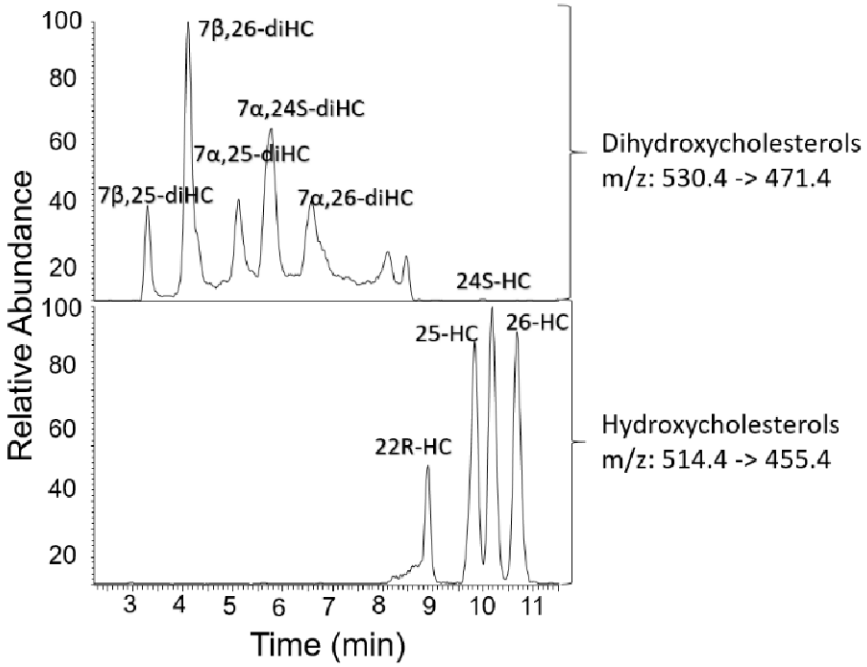

Figure 5 Chromatograms for all nine oxysterols included in this study. Separation is achieved in 11 minutes, and the total run-time for the method including on-line sample cleanup is 21 min. In this figure, a standard solution with a concentration of 500 pM is injected. Cell medium was added at the beginning of the sample preparation for matrix matching. Monitoring of 13C-labelled cholesterol products was also performed; no autoxidation was detected throughout the study.

Healthy liver spheroids/organoids secrete 26-HC

Applying our method we could detect and quantify 26-HC secreted from 20 liver organoids per sample (*Figure 6*). Medium from both primary human spheroids (two different donors; PHH-1 and PHH-2) and hESC/hiPSC-derived liver organoids (three different cell lines; HLC-1, HLC-2, and HLC-3) contained quantifiable levels of 26-HC (see *Figure 6* for representative chromatograms and *Figure 7* for quantitative data). The presence of 26-HC documents sufficient activity of the enzyme CYP27A1 to render detectable levels of secreted 26-HC. The amounts of 26-HC secreted from control/healthy HLCs are generally less than that secreted from the PHH, which is in accordance with a generally lower level of enzyme activity in HLC than in PHH [25]. In contrast to 26-HC, 25-HC, and 24S-HC were detectable only in some of the samples and at levels that are close to the detection limit. The above-specified dihydroxycholesterols were not detected in any of the samples (Figure 6).

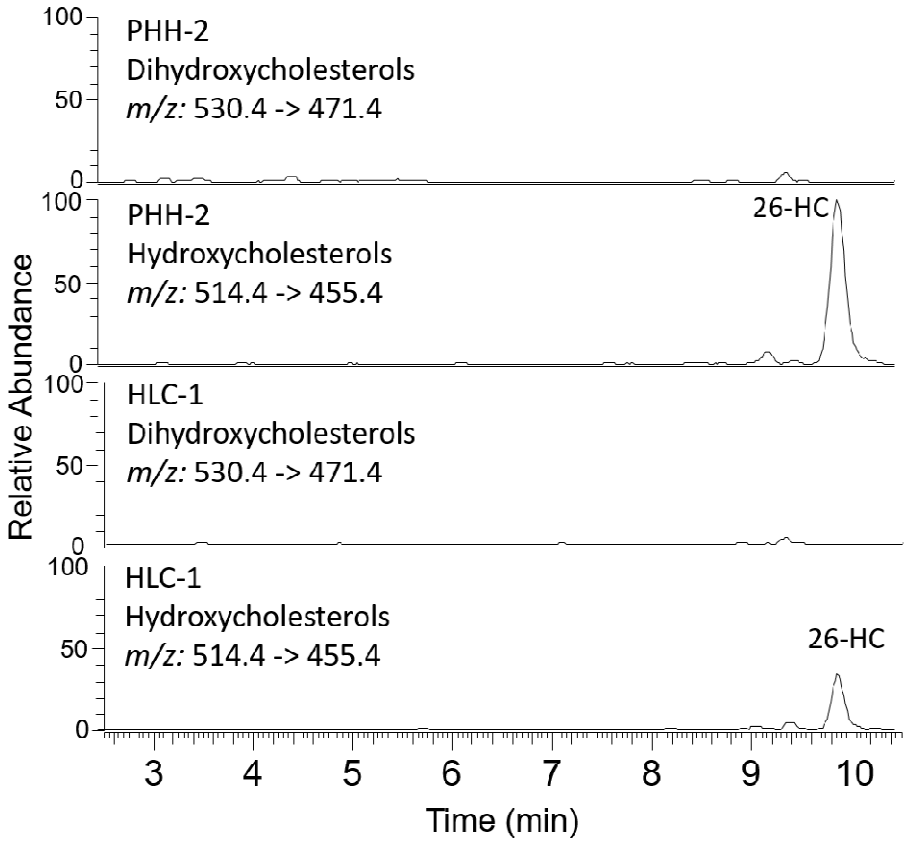

Figure 6 Extracted ion chromatograms for untreated PHH and HLC. For both the m/z- transitions 530.4 → 471.7 and 514.4 → 455.4 is shown, corresponding to the dihydroxycholesterols and hydroxycholesterols, respectively.

Steatotic liver spheroids/organoids secrete increased levels of oxysterols

To analyse the secretion of oxysterols under pathological conditions, we established a model of hepatic steatosis *in vitro* using spheroids generated from primary human hepatocytes (PHH) and organoids generated from hESC/hiPSC-derived hepatocyte-like cells (HLC) (Figure 7A). The liver spheroids/organoids were characterized by an accumulation of lipids as visualized by Nitrile Red staining, while preserving albumin expression (Figure 7B). Moreover, steatotic PHH and HLC were characterized by a statistically significant upregulation of the expression of sterol regulatory element-binding protein 1 (*SREBP-1*) and a consistent trend of increased expression of HMG-CoA reductase - a rate-limiting enzyme of cholesterol biosynthesis (Figure 7C). We detected no statistically significant difference in the expression of enzymes responsible for oxysterol oxidation (*CYP7A1* and *CYP27A1*) in steatotic PHH and HLC.

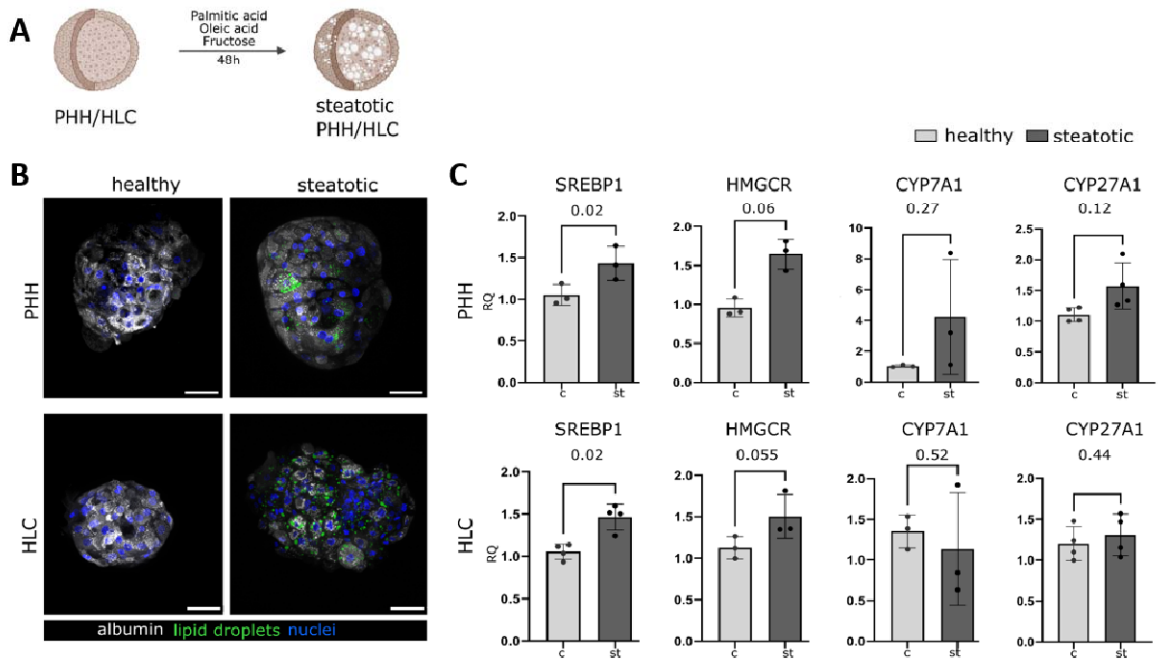

Figure 7 Characterization of hepatic steatosis models using PHH and HLC. A) Schematic presentation of the protocol for inducing hepatic steatosis in vitro. b) Representative images of whole-mount immunofluorescent staining of albumin (white) and cytoplasmic lipids (green) in PHH and HLC. Scale bar 50 µm. c) gene expression in PHH (upper row) and in HLC (low row) after 48 h of steatosis induction. Results represent mean ± SD; n = 3 samples of PHH (N = 2 and more technical replicates for each), and n = 3 cell lines of HLC (N = 3 or more technical replicates for each). A two-tailed, paired t-test is used for the statistics.

Oxysterol levels in media of healthy control spheroids/organoids and steatotic liver spheroids/organoids were subsequently compared. Independent of the spheroids/organoids or experimental repeat, we found a significant difference in the amount of 26-HC secreted from steatotic PHH and HLC compared to controls (*Figure 7A*). While 26-HC was clearly the dominant oxysterol isomer in PHH and HLC, a majority of the steatotic PHH and HLC samples also contained detectable traces of 25-HC and 24S-HC. This suggests sufficient activity of CH25H and CYP46A1 in addition to CYP27A1 in the spheroids/organoids to reach detectable levels of these hydroxycholesterol analytes (Figure 7B). Elevated 26-HC levels detected in steatotic liver spheroids/organoids are in accordance with observations by Ikegami et al. where elevated levels of 26-HC in serum from NAFLD patients [9] was demonstrated. Our findings also support that levels of secreted oxysterols may differ from oxysterols that are retained in cells or liver tissue, if compared to the oxysterols Raselli et al found at elevated levels in liver biopsies from NASH-patients and liver tissue from murine feeding models [10]. In contrast to healthy liver

389 spheroids/organoids, dihydroxycholesterols 7β,25-diHC, 7α,25-diHC, 7α,26-diHC, and 7β,26-
390 diHC were detected in steatotic liver spheroid/organoid samples (*Figure 7**C***). In addition, 7α26-
391 HC was present in amounts close to quantification limits in the HLC_2 samples (Figure 8C),
392 demonstrating low but functional expression and activity of CYP7B1. These data indicate a
393 fingerprint of hydroxycholesterols and dihydroxycholesterols that are secreted by the steatotic
394 liver spheroids/organoids and that differentiates them from healthy liver spheroids/organoids.

395

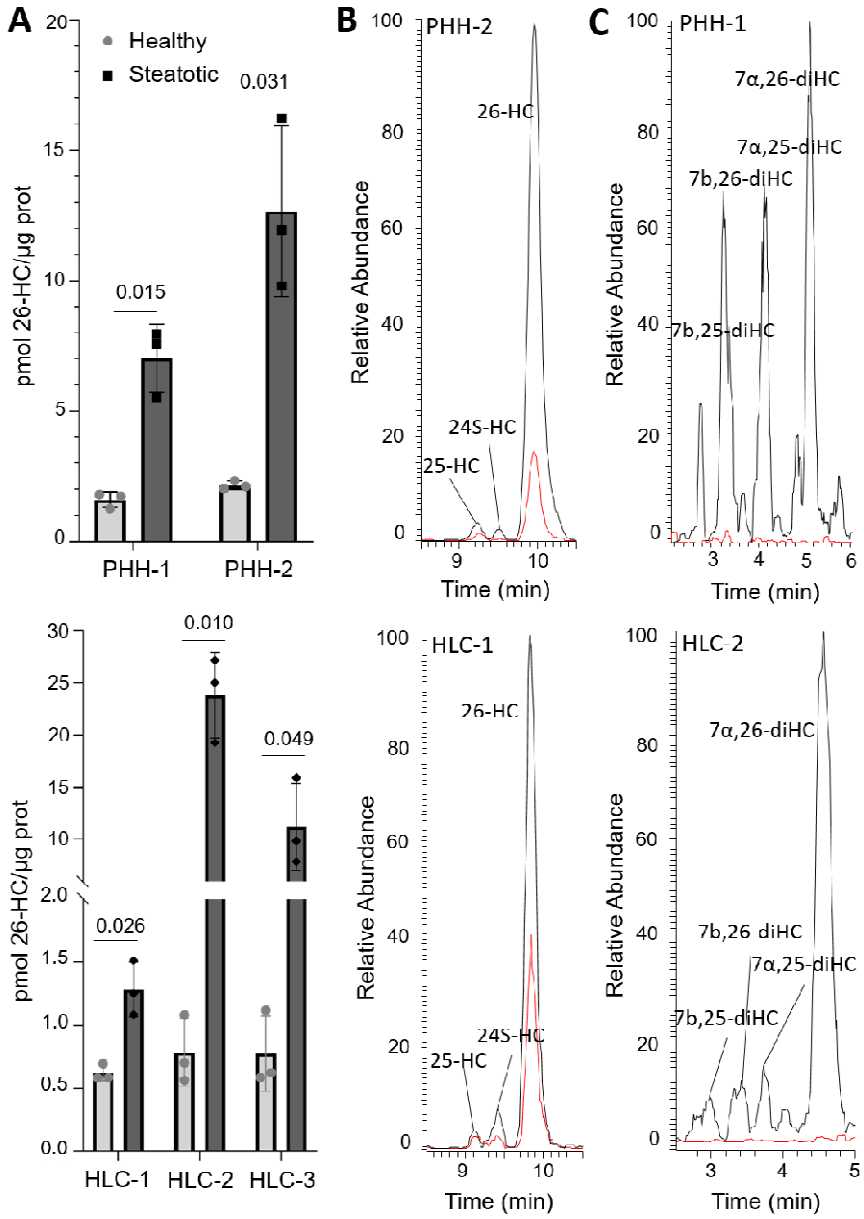

Figure 7 Oxysterol secretion of liver spheroids/organoids. A) The amounts of 26-HC secreted from healthy and steatotic liver spheroids/organoids. The above figure shows two different PHH cell lines, while the below shows three different HLC cell lines. Results represent mean ± SD; n=3 for each cell line. A multiple, unpaired t-test is used to compare healthy and steatotic spheroids/organoids, and P-value is shown for each. B) Representative chromatogram for hydroxycholesterols secreted from healthy (red line) and steatotic (black line) spheroid/organoid samples, PHH (above) and HLC (below), m/z = 514.4 -> 455.4 (hydroxycholesterols). The abundances are normalized to steatotic samples. C) Representative chromatograms for dihydroxycholesterols secreted from healthy control (red line) and steatotic (black line) samples, PHH (above) and HLC (below), m/z = 530.4 -> 471.4. Abundance is normalized to steatotic samples.

407 **The effect of oxysterols on hepatic stellate cells**

408 The transition between NAFL (steatosis) and NASH (steatohepatitis) is orchestrated by HSCs,
409 which are the main secretors of extracellular matrix and important actors in the recruitment of
410 circulating monocytes [26]. In the homeostatic liver, HSCs exhibit a quiescent phenotype but in
411 response to hepatic damage, including steatosis, HSCs are activated and release extracellular
412 matrix components like collagens as well as pro-inflammatory cytokines such as chemokine (C-C
413 motif) ligand 2 (CCL2) [26-28]. Stem cell-derived HSCs differentiated from one hESC line and two
414 hiPSC lines were used to investigate the impact of cholesterol, 25-HC and 26-HC on the
415 quiescent state of HSCs. 7α,26-diHC, which was strongly released by both steatotic PHH and
416 HLC, was not commercially available and was not evaluated.

417 Quiescent-like HSCs were treated with cholesterol, 25-HC, or 26-HC (Figure 9A) and mRNA
418 expression detected with RT-qPCR analysis found a consistent trend of *CCL2* downregulation in
419 response to the treatment with 26-HC (Figure 9B). In the same cells, expression of genes
420 associated with the activation of HSCs (*ACTA2*, encoding α-smooth muscle actin, and *COL1α1*,
421 encoding type I collagen) were not altered by cholesterol, 25-HC, or 26-HC (Figure 9B).
422 Moreover, treatment with cholesterol, 25-HC or 26-HC did not appear to prevent or enhance
423 the TGF-β-induced upregulation of *CCL2*, *ACTA2* and *COL1α1* with the exception of minor
424 variations (Figure 9C).

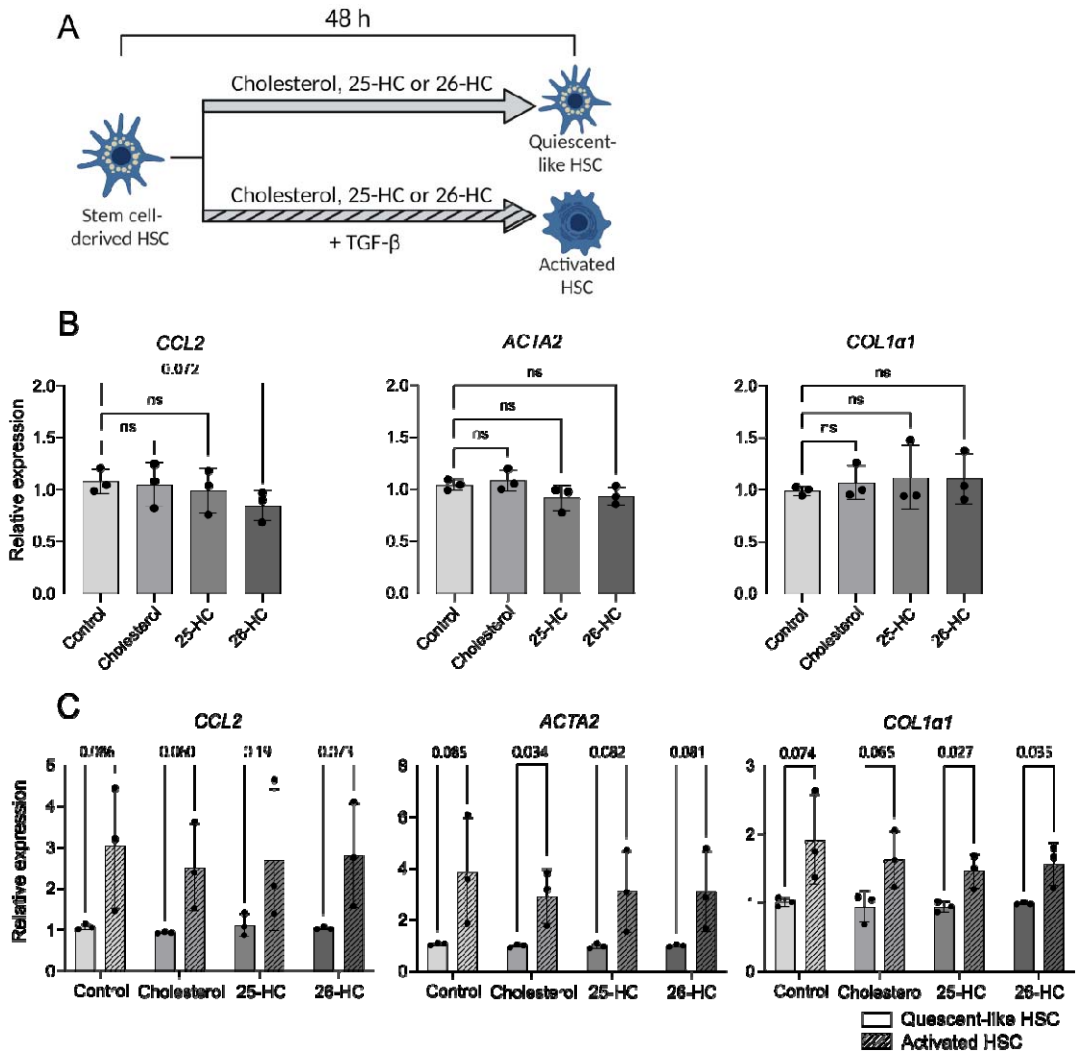

Figure 8. The effect of cholesterol, 25-HC and 26-HC on HSCs. A) Schematic representation of the experiment. HSCs were treated with 50 µM cholesterol, 100 nM 25-HC or 100 nM 26-HC for 48 hours in the presence and absence of activation-inducing stimuli by 25 ng/mL TGF-β. B) Gene expression of activation-associated genes ACTA2, COL1α1 and CCL2 in response to treatment with cholesterol, 25-HC and 26-HC. Gene expression levels were normalized to the control condition. C) Upregulation of activation-associated genes ACTA2, COL1α1 and CCL2 in response to activation-inducing stimuli by TGF-β. Gene expression levels were normalized to "Quiescent-like HSC" samples of each condition. Results represent mean SD, n = 3 independent differentiations of three different PSC lines, three biological replicates for each point. GAPDH was used as the housekeeping gene in all RT-qPCR analyses. Statistical tests: For figure B, a one-way ANOVA with Dunnett's multiple comparison test comparing control and treatment; for figure C, unpaired, two-tailed t-tests comparing "Quiescent-like HSC" and "Activated HSC" in each group.

Collectively, the results suggest that 26-HC may exert an anti-inflammatory signal on quiescent HSCs and consequently might have an impact on the progression of NAFL to NASH, as evident by consistent trends in lowered expression of *CCL2*. However, the effect was absent in TGF-β-activated HSCs. These observations are consistent with existing literature that implicates 26-HC in the attenuation of NAFL [29].

440 ## CONCLUSION

441 As a new analytical approach, we have introduced sterolomics to organoids, an emerging tool
442 for e.g. replacing animal models in biomedical research. Our targeted LC-MS method for
443 determination of Girard T derivatized oxysterols reveal that organoids secrete oxysterols, and
444 26-HC and diHCs were significantly elevated in steatotic samples. Our results, using human liver
445 organoid models, support previous findings based on human serum samples, adding arguments
446 to the validity of human liver organoids as disease models. The association of specific oxysterols
447 with a potential anti-inflammatory role calls for further investigations of oxysterols in NAFLD
448 disease progression. As the elevated oxysterol levels do not correspond with mRNA findings in
449 steatotic spheroids/organoids it shows the importance of direct measurements of metabolites.

450 ## ACKNOWLEDGEMENTS

451 This work was supported by the Research Council of Norway through its Centre of Excellence
452 scheme, project number 262613, and project number: 295910 (National Network of Advanced
453 Proteomics Infrastructure). Support was also provided by UiO:Life Science and the Olav Thon
454 Foundation.

455

456 1. Moore, J.B., *From sugar to liver fat and public health: systems biology driven studies in*
457 *understanding non-alcoholic fatty liver disease pathogenesis.* Proceedings of the
458 Nutrition Society, 2019. **78**(3): p. 290-304.
459 2. Younossi, Z.M., *Non-alcoholic fatty liver disease–a global public health perspective.*
460 Journal of hepatology, 2019. **70**(3): p. 531-544.
461 3. Le, M.H., et al., *2019 global NAFLD prevalence-A systematic review and meta-analysis.*
462 Clinical Gastroenterology and Hepatology, 2021.
463 4. Stefan, N., H.-U. Häring, and K. Cusi, *Non-alcoholic fatty liver disease: causes, diagnosis,*
464 *cardiometabolic consequences, and treatment strategies.* The Lancet Diabetes &
465 Endocrinology, 2019. **7**(4): p. 313-324.
466 5. Gallage, S., et al., *A researcher's guide to preclinical mouse NASH models.* Nature
467 Metabolism, 2022: p. 1-18.
468 6. *Method of the Year 2017: Organoids.* Nature Methods, 2018. **15**(1): p. 1-1.
469 7. Kozyra, M., et al., *Human hepatic 3D spheroids as a model for steatosis and insulin*
470 *resistance.* Scientific reports, 2018. **8**(1): p. 1-12.
471 8. Jia, W., et al., *Targeting the alternative bile acid synthetic pathway for metabolic*
472 *diseases.* Protein & cell, 2021. **12**(5): p. 411-425.
473 9. Ikegami, T., et al., *Increased serum liver X receptor ligand oxysterols in patients with non-*
474 *alcoholic fatty liver disease.* Journal of gastroenterology, 2012. **47**.
475 10. Raselli, T., et al., *Elevated oxysterol levels in human and mouse livers reflect nonalcoholic*
476 *steatohepatitis[S].* Journal of Lipid Research, 2019. **60**(7): p. 1270-1283.
477 11. Griffiths, W.J. and Y. Wang, *Oxysterol research: a brief review.* Biochemical Society
478 Transactions, 2019. **47**(2): p. 517-526.
479 12. Lehmann, J.M., et al., *Activation of the nuclear receptor LXR by oxysterols defines a new*
480 *hormone response pathway.* Journal of Biological Chemistry, 1997. **272**(6): p. 3137-3140.
481 13. Becares, N., et al., *Impaired LXRα Phosphorylation Attenuates Progression of Fatty Liver*
482 *Disease.* Cell Reports, 2019. **26**(4): p. 984-995.e6.
483 14. Pandak, W.M. and G. Kakiyama, *The acidic pathway of bile acid synthesis: Not just an*
484 *alternative pathway.* Liver research, 2019. **3**(2): p. 88-98.
485 15. Fakheri, R.J. and N.B. Javitt, *27-Hydroxycholesterol, does it exist? On the nomenclature*
486 *and stereochemistry of 26-hydroxylated sterols.* Steroids, 2012. **77**(6): p. 575-577.
487 16. Busek, M., et al., *Pump-less, recirculating organ-on-a-chip (rOoC) platform.* Lab on a
488 Chip, 2023.
489 17. Coll, M., et al., *Generation of hepatic stellate cells from human pluripotent stem cells*
490 *enables in vitro modeling of liver fibrosis.* Cell stem cell, 2018. **23**(1): p. 101-113. e7.
491 18. Vallverdú, J., et al., *Directed differentiation of human induced pluripotent stem cells to*
492 *hepatic stellate cells.* Nature Protocols, 2021. **16**(5): p. 2542-2563.
493 19. Schindelin, J., et al., *Fiji: an open-source platform for biological-image analysis.* Nature
494 methods, 2012. **9**(7): p. 676-682.
495 20. Roberg-Larsen, H., et al., *Highly automated nano-LC/MS-based approach for thousand*
496 *cell-scale quantification of side chain-hydroxylated oxysterols [S].* Journal of lipid
497 research, 2014. **55**(7): p. 1531-1536.
498 21. Griffiths, W.J., et al., *Discovering oxysterols in plasma: a window on the metabolome.*
499 Journal of proteome research, 2008. **7**(8): p. 3602-3612.

500 22. Roberg-Larsen, H., et al., *Highly automated nano-LC/MS-based approach for thousand*
501 *cell-scale quantification of side chain-hydroxylated oxysterols.* J Lipid Res, 2014. **55**(7): p.
502 1531-6.
503 23. Solheim, S., et al., *Fast liquid chromatography-mass spectrometry reveals side chain*
504 *oxysterol heterogeneity in breast cancer tumour samples.* The Journal of Steroid
505 Biochemistry and Molecular Biology, 2019. **192**: p. 105309.
506 24. Roberg-Larsen, H., et al., *High sensitivity measurements of active oxysterols with*
507 *automated filtration/filter backflush-solid phase extraction-liquid chromatography–mass*
508 *spectrometry.* Journal of Chromatography A, 2012. **1255**: p. 291-297.
509 25. Graffmann, N., B. Scherer, and J. Adjaye, *In vitro differentiation of pluripotent stem cells*
510 *into hepatocyte like cells-basic principles and current progress.* Stem Cell Research, 2022:
511 p. 102763.
512 26. Tsuchida, T. and S.L. Friedman, *Mechanisms of hepatic stellate cell activation.* Nature
513 reviews Gastroenterology & hepatology, 2017. **14**(7): p. 397-411.
514 27. Kitto, L.J. and N.C. Henderson, *Hepatic stellate cell regulation of liver regeneration and*
515 *repair.* Hepatology Communications, 2021. **5**(3): p. 358-370.
516 28. Tacke, F., *Targeting hepatic macrophages to treat liver diseases.* Journal of hepatology,
517 2017. **66**(6): p. 1300-1312.
518 29. Bieghs, V., et al., *The cholesterol derivative 27-hydroxycholesterol reduces steatohepatitis*
519 *in mice.* Gastroenterology, 2013. **144**(1): p. 167-178. e1.

520